AD-A056 221 ROYAL AUSTRALIAN NAVY RESEARCH LAB EDGECLIFF F/G 8/3
MEASUREMENT OF SURFACE CURRENTS AROUND AN EDDY.(U)
OCT 77 C S NILSSON
UNCLASSIFIED RANRL-TN-5/77 NL

END
DATE FILMED
8 -78
DDC

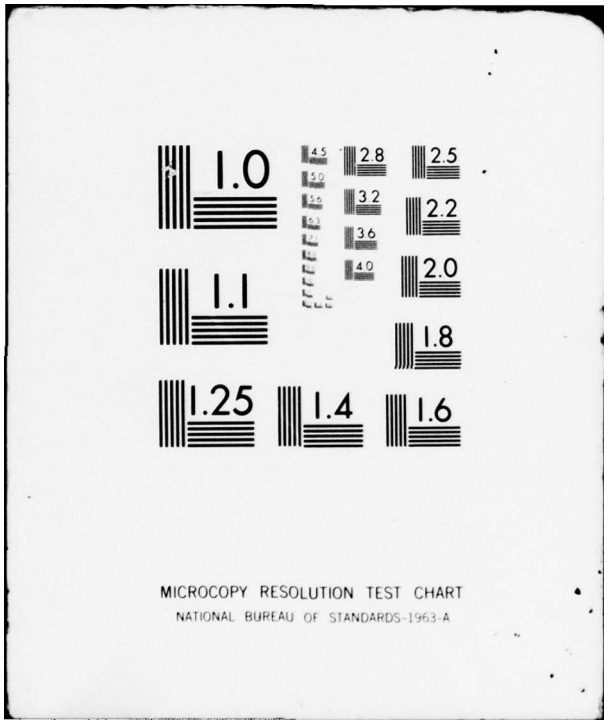
1.0
1.1
1.25
1.4
1.6
1.8
2.0
2.2
2.5
2.8
3.2
3.6
4.0
4.5
5.0
MICROCOPY RESOLUTION TEST CHART
NATIONAL BUREAU OF STANDARDS-1963-A

UNCLASSIFIED

LEVEL II

AR Number: AR-001-010

(12)

DEPARTMENT OF DEFENCE
DEFENCE SCIENCE AND TECHNOLOGY ORGANISATION
R.A.N. RESEARCH LABORATORY
EDGECLIFF, N.S.W.

RANRL TECHNICAL NOTE No. 5/77

MEASUREMENT OF SURFACE CURRENTS AROUND AN EDDY (U)

BY

C. S. NILSSON

APPROVED FOR PUBLIC RELEASE

COPY No. 53

OCTOBER 1977

UNCLASSIFIED

UNCLASSIFIED

DEPARTMENT OF DEFENCE

RAN RESEARCH LABORATORY

RANRL TECHNICAL NOTE NO. 5/77

MEASUREMENT OF SURFACE CURRENTS AROUND AN EDDY (U)

C.S. Nilsson

S U M M A R Y

A closed eddy off East Australia was surveyed during the period 8-13 December 1974 by HMAS KIMBLA. A comparison of dead reckoning data with a series of satellite navigation fixes yielded a series of total current measurements around the eddy. These observed values are compared to the current vectors expected from the measured dynamic height topography. The comparison gives the average enhancement factor applicable to normal geostrophic current due to centrifugal force around the eddy. The factor 1.25 is shown to be consistent with the eddy dimensions and related to the Rossby radius of deformation. The data are also analysed for a mean barotropic flow, giving a value for the mean eddy motion of 5 ± 5 cm.sec^{-1} to $045^{o} \pm 45^{o}$.

APPROVED FOR PUBLIC RELEASE

POSTAL ADDRESS: The Superintendent, RAN Research Laboratory
Box 706, Darlinghurst, NSW, 2010

UNCLASSIFIED

DOCUMENT CONTROL DATA SHEET

Security classification of this page: UNCLASSIFIED

1. **DOCUMENT NUMBERS:**
   a. AR Number AR- 001-010
   b. Document Series and Number: RANRL Technical Note
   c. Report Number: 5/77

2. **SECURITY CLASSIFICATION:**
   a. Complete document: UNCLASSIFIED
   b. Title in isolation: UNCLASSIFIED
   c. Summary in Isolation: UNCLASSIFIED

3. **TITLE** (6) MEASUREMENT OF SURFACE CURRENTS AROUND AN EDDY (U)

4. **PERSONAL AUTHOR(S):** (10) [redacted], Carl S. NILSSON

5. **DOCUMENT DATE:** (11) October 1977 (14) RANRL-TN-5/77

6. **TYPE OF REPORT AND PERIOD COVERED:** (9) Technical Note.

7. **CORPORATE AUTHOR(S):**
   RAN Research Laboratory
   P.O. Box 706
   DARLINGHURST NSW 2010

8. **REFERENCE NUMBERS:**
   a. Task: ANZUS Eddy - 76/065
   b. Sponsoring Agency: NSA
   c. Approved: W.F. Hunter

9. **COST CODE:** (12) 27 P.

10. **IMPRINT** (Publishing establishment)
    RAN Research Laboratory

11. **COMPUTER PROGRAM(S):** (Title(s) and Language(s))

12. **RELEASE LIMITATIONS** (of the document in addition to the distribution list)

AUSTRALIA: APPROVED FOR PUBLIC RELEASE

OVERSEAS: N.O. [ ] P.R. [1] A [ ] B [ ] C [ ] D [ ] E [ ]

13. **ANNOUNCEMENT LIMITATIONS** (of the information on this page):
NO LIMITATION

14. **DESCRIPTORS:**
OCEAN CURRENTS
OCEANOGRAPHIC SURVEYS
EDDIES

15. **COSATI CODES:**
0803
0810
2004

16. **SUMMARY/ABSTRACT:** A closed eddy off East Australia was surveyed during the period 8-13 December 1974 by HMAS KIMBLA. A comparison of dead reckoning data with a series of satellite navigation fixes yielded a series of total current measurements around the eddy. These observed values are compared to the current vectors expected from the measured dynamic height topography. The comparison gives the average enhancement factor applicable to normal geostrophic current due to centrifugal force around the eddy. The factor 1.25 is shown to be consistent with the eddy dimensions and related to the Rossby radius of deformation. The data are also analysed for a mean barotropic flow, giving a value for the mean eddy motion of 5 (± 5) cm.sec^{-1} to 045° (± 45°).

(± 5) → + OR − CM/SEC; (± 45°) → + OR − deg; ABSTRACT

406 608

ii

UNCLASSIFIED
Security classification of this page

hC

DISTRIBUTION (Cont'd)

	Copy No.
United States	
Defence Documentation Centre (via DISB)	53-64
Counsellor, Defence Science, Washington (CONDS)	65
Mr P. Scully-Power, Naval Underwater Systems Center, New London	66
New Zealand	
Superintendent, Defence Scientific Establishment	67
Dr R. Banister, Defence Scientific Establishment	68

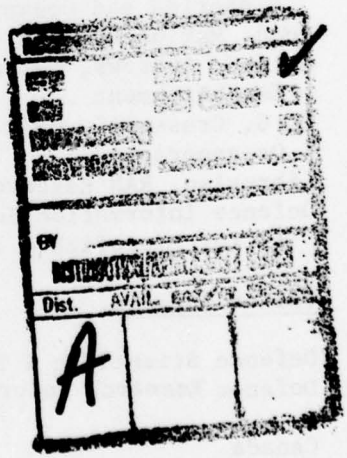

DISTRIBUTION

	Copy No.
Australia	
Chief Defence Scientist	1-2
Chief of Naval Technical Services	3
Chief of Naval Materiel	4
Defence Science and Technology Committee, Secretary	5
Director General Naval Operational Requirements	6
Executive Controller, Australian Defence Scientific Service	7
Superintendent, Defence Science Administration	8
Assistant Secretary, Scientific and Technical Information	9
Head, Laboratory Programmes	10
Controller, Service Laboratories and Trials Division	11
Director, Programming and Trials Executive	12
O.I.C. RAN Trials and Assessing Unit	13-14
Naval Scientific Adviser	15-16
Superintendent, RAN Research Laboratory	17
Head, Engineering Development Establishment	18
Chief Superintendent, Aeronautical Research Laboratories	19
Chief Superintendent, Materials Research Laboratories	20
Superintendent, Physical Chemistry Division, Materials Research Laboratories	21-22
Superintendent, PMD Division, Weapons Research Establishment	23
Flag Officer Commanding, HM Australian Fleet	24
Flag Officer Commanding, East Australia Area	25
Commanding Officer, HMAS KIMBLA	26-27
Defence Library, Campbell Park	28
Senior Librarian, Weapons Research Establishment	29-30
Chief, CSIRO Division of Fisheries and Oceanography	31
Head, Physics and Chemistry Group, CSIRO Division of Fisheries and Oceanography	32-33
Head, Marine Physics Group, Weapons Research Establishment	34-35
Mr J.C. Andrews, Marine Physics Group, Weapons Research Establishment	36
Dr G. Cresswell, CSIRO Division of Fisheries and Oceanography	37
Librarian, RAN Research Laboratory	38-47
Defence Information Services Branch (1 for Microfiche, 1 for National Library)	48-49
United Kingdom	
Defence Scientific & Technical Representative	50
Defence Research Information Centre (via DISB)	51
Canada	
Defence Scientific Information Service (via DISB)	52

CONTENTS

TABLES

LIST OF FIGURES

1. INTRODUCTION

The purpose of this study was to demonstrate that the surface currents estimated from the observed baroclinic structure of a closed mesoscale eddy were in fact representative of the actual currents encountered. This was done following an experiment in which the prime objective was simply to find such an eddy and determine whether or not the structure was closed. No direct current measurements were made with either in-situ meters or a towed geomagnetic electrokinetograph (GEK). A set of fixes taken with satellite navigation and the dead reckoning (DR) log of the ship comprised the only data available. To make matters more difficult the ship (HMAS KIMBLA) was not fitted with a speed log. The bridge log, hourly sums of engine revolutions and the meteorological log were the only data from which to estimate speed and DR. Given these limitations the analysis is nevertheless worthwhile. Currents were estimated from the set of the ship, i.e. from the vector differences between the calculated progress of the ship through the water and the observed progress over the ground.

2. ESTIMATION OF DEAD-RECKONING DATA

A theoretical model of ship's speed through the water as a function of engine revolutions and weather conditions was constructed to best fit the data from this particular experiment, Trial 19/74. A detailed account of this model has been given elsewhere (Nilsson, 1977) and only an outline need be given here. Briefly, the following effects were allowed for: retardation of ship's speed due to waves and swell (taking into account the relative angle of incidence), the increase in drag due to applied rudder (particularly in beam winds) and the actual push received from winds and sea. This push affected both the forward speed and also produced a normal component, i.e. leeway. The model was constrained to use only those data normally recorded by the ship's officers every four hours. The pertinent data consisted of sea state, wind (absolute) velocity and swell height and direction. No data on swell and wave periods were available. Figure 1 shows the calculated variation of speed v_1 (in the direction of ship's head) as a function of wind velocity and relative heading. This function has been calculated using the assumptions that wind, waves and swell all come from the same direction, that wave height h_w is proportional to wind speed w (given by $h_w(m) = 0.06\ w\ (kn)$) and further-

more, that swell height is twice the wave height. These two relationships provided a reasonable first order fit to the weather data on Trial 19/74 (8-13 December 1974). Figure 2 shows a plot of the ship's track for Trial 19/74. A total of 66 fixes were obtained from the satellite navigation system during the course of the trial (114 hr). The fixes of significance to this work are lettered. Associated with each labelled fix is a figure giving the number of hours into the trial starting from 0001 hrs(Time Zone K) on 8 December 1974. A list of the observed weather data is given in the Appendix. Figure 3 shows the dynamic topography of the area, derived from Expendable Bathythermograph (XBT) data taken during the trial. The values of dynamic height (0 - 900 m) were calculated by Andrews (unpub.) using a synthetic salinity profile (Andrews 1976). The expected geostrophic currents are inversely proportional to the contour spacing.

Now, the determination of the model parameters for ship's speed rested on two propositions. Firstly, that the surface currents over the legs CDEF were small enough for the net effect to be ignored. Secondly, that the average surface current over the leg RS equalled that over the leg ST. The reasonableness of these propositions can be judged by referring to Figure 3, bearing in mind that a topographic gradient of 10 dyn. cm (0/900 m) per 18.5 km (10.0 n miles) is estimated to produce a surface current of 0.75 m sec^{-1} - see Section 5.

It was assumed that the ship's speed in smooth water, v_o, was linearly related to engine revolutions, n, by

$$v_o = \frac{n}{K} \qquad .....(1)$$

The value of K was one of the most important parameters to be determined. This was done as follows: the weather at the start of the trial was relatively light (winds $\lesssim$ 16 kn) from varying directions until point E was reached, after which the wind freshened to 30 kn from 010° around point E', with sea and swell reaching 1.8 m (6 ft) and 3.7 m (12 ft) respectively from the same direction. After G the wind quietened and came in from the south. During legs RST the winds were again less than 16 kn from varying directions. Thus, variations in the parameters of the model only had a small effect on the calculated progress over legs RST, but a considerable effect over the leg EF, particularly as the wind and sea were almost head on at the time.

In view of the above, an iterative procedure was adopted to fit the various parameters to the data. First estimates were made and the set of the ship calculated along the various legs. If the data and model were perfect, the calculated set between successive fixes would be due to surface current plus any net error in the fixes. This calculated set has been termed the 'drift' in this discussion. In practice, this will also contain errors in the calculated dead reckoning (DR) data. The value of K (Eqn (1)) was adjusted to equalize the magnitude of the drift over the legs RS and ST. Now, with respect to the legs CDEF, errors in calculated ship's speed will show up directly in the comparison between distance travelled through the water, D_w, and distance travelled over the ground, D_g assuming no net effect due to surface currents. The criterion for the model was to minimise $\sum(D_w - D_g)$ over the three legs CD, DE and EF, separately and totally. Having adjusted the model appropriately, the drift over RST was recalculated, K readjusted and so on. This process converged after a few cycles leading to K = 15.0 ± 0.2 r.p.m./kn - a value identical to that traditionally used by HMAS KIMBLA's officers. The drifts during legs RS and ST are 0.74 m sec^{-1} at 290^{o} and 288^{o} true respectively. The dynamic topography suggests a mean current of 0.8 - 0.9 m/sec^{-1} at 285^{o} true, so the calculated directional data (for which there were no direct constraints) are most encouraging.. However, close examination of the data suggests that in general the errors in calculated ship's speed is too large for useful determination of current components parallel to the ships' track whenever the wind speed exceeded 20 kn. The drift component normal to the ship's track is still useful, however, in cases such as that of leg GH, where the expected current is close to normal to the ship's track.

3. EXPECTED ERRORS

Before comparing the observed and expected current magnitudes, we need to bear in mind the expected errors in the measurements. The satellite navigation (single frequency) system should give fixes with a position error ≃ 0.4 n. mile. The larger error component will generally be along the ship's track, due to some uncertainty in ship's speed. However, for fixes obtained with the satellite at high elevation, the error is likely to be greatest in longitude. The mean time between end points used in the determination of drift values is 3.3 hr, so on the average we could expect errors

of about 0.15 kn (0.07 m sec^{-1}) in each component of drift due to fixing errors. Now, with respect to the drift component parallel to the ship's course, the error in calculated speed through the water will certainly exceed that, being more like 0.3 kn (a rough estimate) in mild weather and considerably more once the weather rises. A bias of only 1^{o} in steering also leads to an apparent normal component of drift of 0.15 kn, so errors of, say, twice this may not be uncommon.

Thus, in mild weather we may expect 0.2 - 0.3 kn error in apparent current (drift) speed normal to the ship's course and 0.4 - 0.5 kn parallel to the ship's course. Once the wind rises, these errors will increase, particularly those parallel to the ship's course. Under such conditions it will generally be more appropriate to use only the normal drift component.

4. DYNAMIC HEIGHT TOPOGRAPHY

It was necessary to obtain the dynamic height topography of the area with respect to some reference depth in order to derive the expected surface currents. Hamon (1965), in earlier work on the East Australian current, assumed 1300 m for the depth of no motion. This implies that the structure above that depth accounts for all the variability in surface motion. However, after some studies using free-floating pingers at various depths, he (Hamon, 1970) concluded that the reference depth needs to be greater,say 2000 m or more. There is little doubt, though, that most of the surface currents can be adequately described with reference to a lesser depth. Such dynamic height topography has been obtained in the past on a much coarser grid scale by using data from Nansen casts. The specific volume anomaly is obtained from water samples taken at specific depths and integrated upwards to the surface from, say, 1300 m.

We were not able to take Nansen casts during Trial 19/24, but in any case the time required for such work precluded their use as the principal tool in obtaining a quasi-synoptic map of the dynamic height topography on as fine a scale as we required. Instead, XBT data were used to obtain the dynamic height structure (0/900 m) shown in Fig. 3 . The depth was limited to 900 m by the XBT probes. The values of dynamic height were obtained in the following way: at the time the only XBT probes available were the type T4 (Plessey-Sippican) nominally limited to 450 m depth. Realizing from previous work

(Andrews and Scully-Power, 1976) that the eddy structure extended below 450 m, some T4 probes were modified by rewinding nearly 500 m of the wire from the launcher spool (in each probe) to the probe spool. Indeed, this operation was performed on ship-board as the trial progressed, using an electric drill, and much care. Probes so modified are slightly heavier at launch and allowance has to be made for their slightly greater rate of descent (theoretically 470 m in 71 sec compared to 450 m for a normal T4 probe). A comparison of data taken with both modified and normal probes verified this difference. A total of > 30 deep probes were successfully used in the course of Trial 19/74. Some of them gave data to over 1000 m, most of them to more than 900 m.

Now, there exists a close correlation between temperature and salinity for subsurface Tasman Sea waters so it was possible to calculate the dynamic height anomalies using a synthetic salinity profile (see Andrews, 1976) from all the XBT data. The values of D(0/900 m) from the modified probes could then be correlated with the values of D(0/450 m). The correlation was extremely close, the correlation coefficient being 0.995 from 17 profiles with the following relationship:

$$D(0/900) = 1.334\ D(0/450) + 17.1 \pm 1.2 \text{ dyn.cm} \qquad .....(2)$$

This relationship was then used to transform all the values of D(0/450) to obtain the topography shown in Fig. 3 . Furthermore, the very good correlation between D(0/900 and D(0/450) indicates that the values of D(0/450) and D(0/900) should also be closely related to D(0/1300).

5. BAROCLINIC SURFACE CURRENTS

In this paper we shall use the term baroclinic current to refer to that component of the actual current which varies over the area and tends asymptotically to zero (by definition) with depth - being effectively zero for all depths greater than the so-called depth of no motion. The other component of the actual current is the barotropic component which is independent of depth and has to be vectorially added to the baroclinic current. In general one expects the baroclinic surface currents around the eddy to be an order of magnitude greater than the barotropic component.

The computation of expected surface currents from the dynamic height topography (0/900 m) shown in Fig 3 requires an assumption of the depth of the

layer of no motion. The dynamic topography has only been calculated with respect of 900 m, whereas Boland and Hamon (1970) found that the East Australian Current (EAC) extends to a depth of at least 2000 m. They adjusted their baroclinic velocity-depth profiles (their Fig.14) to give the same velocity at 1200 m as that from one of their free-floating pingers. This assumes no significant barotropic (depth-averaged) component, an assumption which may be out by perhaps 0.1 m sec^{-1}. From their profiles the actual (baroclinic) surface current speed can be related to the surface speed with respect to 900 m by

$$v(\text{actual}) \simeq 1.15 \times v(0/900\ \text{m}) \qquad \ldots(3)$$

that is, approximately 87% of the actual dynamic topography at the surface is due to the structure between the surface and 900 m. This factor has been used to compute the expected geostrophic current C_g from the contours of Fig. 3 .

There is another consideration with respect to the expected surface current. The curvature of the topographic contours adds a centrifugal component to the usual geostrophic current. From Von Arx (1962), the balance of forces is given by (his Eq. 4-35)

$$\rho \frac{Cm^2}{r} + \text{grad}_h\, p - \rho\, f\, C_m = 0 \qquad \ldots(4)$$

where ρ is the density of sea water,

r is the radius of curvature of the contours,

$\text{grad}_h\, p$ is the horizontal radial component of the total pressure gradient force,

f is the usual Coriolis parameter and

C_m is the tangential (meander) current speed.

Now in the absence of curvature ($r \to \infty$), this reduces to the usual geostrophic equation ($Cm \to C_g$)

$$C_g = \frac{1}{\rho f}\ \text{grad}_h p \qquad \ldots(5)$$

where C_g denotes the geostrophic current speed in the absence of curvature.

Substituting (5) into the appropriate quadratic solution to (4), we obtain

$$C_m = \frac{rf}{2}\left[1 - \left(1 - \frac{4C_g}{rf}\right)^{\frac{1}{2}}\right] \qquad \ldots.(6)$$

Equation (6) illustrates the fact, noted by Von Arx, that in the presence of curvature, the pressure gradient is limited by

$$C_g \leq \frac{rf}{4} \qquad \ldots.(7)$$

Thus pressure gradients (and surface currents in balance) must be small near the centre of an anti-cyclonic eddy, where r is small. Further, when the limiting curvature is reached, the maximum surface current is given by

$$C_m = \frac{rf}{2} \qquad \ldots.(8)$$

when the pressure gradient is such that

$$C_g = \frac{rf}{4}$$

i.e. C_m can have up to twice the value that C_g would have if there were no curvature.

For latitude $34^{o}30'S$, $f = 0.826 \cdot 10^{-4}$ sec^{-1} and for a not uncommon pressure gradient of 1.0 dyn. cm/km, $C_g = 1.21$ m sec^{-1}. From (7) the minimum value the curvature can have is given by

$$r_{min} = \frac{4C_g}{f} \qquad \ldots.(9)$$

which, for this example, gives $r_{min} = 58.6$ km. Under these conditions, the actual current speed would be $C_m = 2.42$ m sec^{-1}. It is apparent that, given the contour spacing and scale of Fig. 3, the enhancement of the normal geostrophic velocity due to curvature should be taken into account when calculating expected surface currents. Indeed, pressure gradients and surface currents around EAC eddies may often reach their limiting values. A case in point apparently occurred in March 1975. An intense southward current flow offshore from Sydney turned east at 36^{o} S. This can be seen in the contours shown by Nilsson, Andrews and Scully-Power, 1977 (their Fig. 4a). The contour spacing increased immediately the stream turned east, as it had to in order to maintain the balance given by Eq.(4).

We can define

$$R = \frac{r_{min}}{r} \quad \text{where} \quad 0 < R \leq 1$$

and (6) reduces to

$$\frac{C_m}{C_g} = \frac{2}{R}(1 - \sqrt{1-R}) \qquad \ldots.(10)$$

The ratio $\frac{C_m}{C_g}$ of meander to geostrophic current speed is shown in Fig. 4 .

6. COMPARISON OF OBSERVED AND EXPECTED SURFACE CURRENTS

Table 1 gives the drift data for the pertinent part of Trial 19/74. The individual legs can be related to the track of Fig. 2 and the topography of Fig. 3; the value of Δt(hr) gives the elapsed time between the appropriate fixes. The 'observed' values comprise drift distance and direction; the mean drift speed v_{dr} is given in knots and m sec^{-1}. In three instances (e.g. leg G-H) only the component of drift normal to the ship's track has been used, because of uncertainty in the ship's forward speed. These are subscripted by $\perp$.

The 'expected' set has been calculated by roughly integrating the stream flow indicated by the contours in Fig. 3 along each leg of the track with respect to time. The resultant expected drift is also given in Table 1. As discussed in the previous section, the geostrophic flow from 0 - 900 m has been enhanced by a factor of 1.15 to arrive at an expected value of C_g. At this stage only the contour spacing has been considered - no enhancement due to curvature has been incorporated. The errors in the individual determinations of observed and expected speeds preclude using each value of v_{dr} as a measure of meander velocity C_m in order to calculate individual values of the ratio R (ref. Eq. (10)). Also, in many cases the radius of curvature varies quite rapidly, so that only mean values over each leg could be obtained anyway. It would be interesting, given a well-defined structure such as this eddy, to correlate a continuous record of current (such as might be obtained by a GEK) with the local pressure gradient and curvature. The residuals would provide information on ageostrophic components and turbulence on the scales down to, say, 2 km.

Before comparing values of drift speed, it is necessary to compare drift directions. The expected flow directions were only estimated to the nearest 5^{o} from Fig. 3; hence the agreement shown in Table 1 is quite good. The median value of the absolute differences is 6^{o} (xcluding the three cases in which only the component normal to the ship's track was used). The mean difference over the 13 comparisons is + 5^{o}, which is not significant. Clearly, we can proceed to compare the absolute speeds.

For this experiment the data must be treated statistically. The data of Table 1 have been divided into two classes: the drift values obtained along the predominantly straight sections of the contours have been labelled 'S', while those obtained on the bends have been labelled 'B'. Class S contains 6 measurements over a total of 27.8 hr, class B contains 10 measurements over 24.6 hr. Working with a sum of a series of drift measurements has the advantage of reducing the overall error. For example, with a sequential set of fixes, the overall fix error is simply the relative error between the first and last fixes. Even if the series is not sequential, we can expect the overall error to quickly become unimportant. A constant under or over-estimation of ship's speed with a non-random ship's track will continue to bias the drift results; but nearly random errors, such as we might reasonably expect from our estimations of ship's speed, will tend to cancel out. Also, instead of using individual values of v_{dr}, it is better to sum the observed drift distances within each class, S or B, and compare these sums with the sums of expected drift distances. This procedure automatically gives the desired weight to each determination obtained over varying intervals of time.

Writing O(d) for observed drift distance and E(d) for $C_g \Delta t$ for each leg, we obtain:

$$\sum_{S} O(d) = 41.0 \text{ n.mi.}, \qquad \sum_{S} E(d) = 43.3 \text{ n.m.}, \qquad \sum_{S} \Delta t = 27.8 \text{ hr}$$

$$\sum_{B} O(d) = 39.2 \text{ m.mi.}, \qquad \sum_{B} E(d) = 33.0 \text{ n.mi.}, \qquad \sum_{B} \Delta t = 24.6 \text{ hr}$$

The ratio $\sum O(d) / \sum E(d) = 0.95$ for class S (the 'straight' sections of the eddy) and gives 1.19 for class B (the 'bends'). For class S, the difference between 0.95 and 1.00 is equivalent to an average over-estimation of ship's speed of $\sim$ 0.1 kn (the ship mostly went around the eddy with the current

stream) or an over estimation of the correct factor relating surface velocity to C_g(0-900m) by 0.06 (i.e. 1.09 should have been used instead of 1.15). Either error is quite feasible. The distribution of the unweighted individual ratios O(d)/E(d) can also be considered for each class of data and for set S is given by 0.97 ± 0.2 . With only 6 values the difference from unity is obviously not significant. For class B, however, the difference is significant. Firstly, the result for class S gives us some confidence concerning both the estimation of ships' speed (in mild weather) and the factor relating C_g(total) to C_g(0-900 m) Secondly, the distribution of individual ratios O(d)/E(d) for class B is given by 1.31 ± 0.46 . With 10 observations, the mean value differs significantly (at 5%) from unity. Our best value of curvature enhancement can probably be obtained by first reconciling the totals of observed and expected drift distances in class S, i.e. along the 'straights'. We shall do this by reducing the multiplicative factor applied to C_g from 1.15 to 1.09. Whether or not this is the true value or the error lies in the estimations of ship's speed or, in fact, the currents are indeed less than theory would indicate by 5%, hardly matters to the following argument. This step reduces $\sum_B$ E(d) to 31.3 n miles. The ratio $\sum_B$ O(d)/$\sum_B$E(d) now gives 1.25 for the time-averaged enhancement due to curvature.

It can be shown that this is consistent with the eddy dimensions: From Fig. 4, the ratio 1.25 for $\left\langle \frac{C_m}{C_g} \right\rangle$ corresponds to $\langle R \rangle = 0.64$. The time-averaged value of C_g over all the track segments listed in Table 1 is 0.71 m.sec^{-1}. This corresponds (from (9)) to $\langle r_{min} \rangle$ = 34 km and $\langle r \rangle$ = 54 km. The N - S dimension of the eddy (which is most appropriate to the measured enhancement) across the maximum current stream (approximately coincident with the ship's track) is about 110 km. One would thus expect an average radius of curvature ≃ 55 km, in excellent agreement with our value of $\langle r \rangle$.

One can consider the Rossby radius of deformation μ as a mesoscale measure of the scale of instability in the ocean. Andrews and Scully-Power (1976) have shown that

$$\mu \simeq k^{-1} \qquad \ldots.(11)$$

where k is the horizontal wave number. According to their model for these eddies, the maximum current speed occurs at a radius of 0.49 x the total eddy radius, R' say. Also, k R' is the first non-zero root of a first order Bessel function, i.e. k = 3.83/R'. Substituting 0.49 R' = $\langle r \rangle$ = 54 km,

we obtain R' = 110 km and, from (11), μ= 29 km. We observe that the value of μ corresponds approximately to the value of $\langle r_{min} \rangle$. Also, these calculations are mostly based on the smaller north-south eddy dimensions, rather than the larger east-west measurement. Andrews and Scully-Power used a slightly larger value for radius R' (124 km) to obtain μ = 32 km, comparing that with the value 40 km derived by Godfrey (1973 and private communication). Indeed, it should be noted that the eddy under study in this paper is probably the same eddy as that studied by Andrews and Scully-Power three months earlier. The intensity seems to have diminished by about 15-20% in the interim, judging from the temperature sections (not shown).

7. THE MEAN BAROTROPIC CURRENT

The question of where the eddy as a whole is going is of considerable interest. The barotropic velocities will be contained in the observed drift values of Table 2. Consider a set of drift measurement taken all around the eddy and suppose there was a mean southward barotropic component. On the eastern edge of the eddy the measured (northward) drift should be diminished and on the western edge the drift should be enhanced. To the first order, the total observed drift will not be affected, but in each case the values of $[O(d) - E(d)]$ should show a southward component. Along the northern and southern boundaries of the eddy, the drift distances would not change appreciably (so long as the barotropic component is small), but again there will be a southward component.

To isolate the mean barotropic component, first reconcile the observed and expected sums of drift distances in each class (the 'straights, S and the 'bends' B). As discussed in the previous section, this can immediately be done for class S by multiplying all the values of C_g in Table 2 by 0.95 . Then the values of C_m (the expected meander speed) can be obtained from each value of C_g in class B by further multiplying by 1.25 . This gives

$$\sum_S O(d) = \sum_S E(d) = 41.0 \text{ n mi.}$$

and

$$\sum_B O(d) = \sum_B E(d) = 39.2 \text{ n mi.}$$

Now sum the drift vectors $\underset{\sim}{d}$ (both observed and expected) for all 16 measures in Table 2. We obtain

$$\sum_{A-Z} \overline{\underset{\sim}{O(d)} - \underset{\sim}{E(d)}} = \begin{pmatrix} 1.6 \\ -.8 \end{pmatrix} \text{ n mi for the north and east components.}$$

This net drift over 52.4 hr is equivalent to a mean barotropic component of 2 cm.sec^{-1} towards 333^{o} true. We need to obtain some idea of the uncertainty of this measure. The ship's track from point J through to point S constitutes a complete circumnavigation of the eddy (around the stream of maximum current) so consider these 8 measures as a separate group. W obtain:

$$\sum_{J-S} \overline{\underset{\sim}{O(d)} - \underset{\sim}{E(d)}} = \begin{pmatrix} 2.2 \\ 3.5 \end{pmatrix} \text{n mi .}$$

This net drift over 32.5 hr gives a value for the mean barotropic current of 7 cm.sec^{-1} towards 058^{o} true. Because of the closed track and mild weather, this is probably our 'best' measure. If we decrease all the expected currents by 10% (a reasonable margin of error) the barotropic current is 5 cm.sec^{-1} towards 074^{o} and if we increase them all by the same factor the barotropic current is 8 cm.sec^{-1} towards 048^{o}. From this group of results we can reasonably determine the net drift of the whole eddy as 5 ± 5 cm.sec^{-1} towards 045^{o} ± 45^{o}. Any drift west of north seems unlikely as the eddy was already very close to, but separated from, the continental shelf.

Values for the apparent drift of the eddy can be sought in another way: some areas of the eddy were traversed twice during the trial, as can be seen in Fig. 2 For example, XBT data were obtained in proximity to points J and S after a hiatus of about 38 hr. Similar proximate data were obtained near points B and P after a gap of 68 hr and near points H and N after 30 hr. In no case did any difficulty obtain in drawing a quasi-synoptic map, such as Fig 3, indicating that the contours themselves were not appreciably in motion over the ground. If we analyse the apparent variations of D(0/900) with latitude over these sections of track, we find that only the data near J and S indicate any apparently significant meridianal movement and that is small (≃ 0.8 n mi. S) and cannot really be regarded as significant. The apparent movements were:

Area	Time lapse	Movement (N)
B-P	68 hr	0 ± 1 cm sec^{-1}
H-N	30	- 2 ± 3
J-S	38	- 1 ± 1

The uncertainties refer only to the actual scatter in the data.

A similar procedure can be followed in the area M-Z to look for any zonal movement. With only two XBT profiles at the end of the track (near Z) to use for comparison, the result must again be regarded with caution. Both profiles, however, indicate an apparent shift of ≈ 3.5 n mi. E over 41 hr, equivalent to an eastwards movement of 5 cm sec^{-1}.

The data on the eastern side of the eddy were obtained with insufficient time lapse (≈ 16 hr) for any reliable measure and no satellite fixes were obtained for over 5 hr immediately preceding point R. Nevertheless, the apparent shift is ≈ 5 n mi. E. This leads one to speculate that the eastwards movement may have been more pronounced at the eastern edge of the eddy and that perhaps this was associated with the east-west orientation of the eddy's long axis.

8. CONCLUSIONS

Despite limited data on ship's speed it has been possible to compare expected currents around an eddy with those measured from the set of the ship. The data do not indicate any overall departure from the currents expected from the dynamic relief estimated to 1300 m, once the theoretical speed enhancement due to centrifugal force is taken into account. The time-averaged value for this enhancement factor in the neighbourhood of the eddy curves was estimated to be 1.25, a value consistent with the dimensions of this eddy. The normal geostrophic current can be enhanced by a factor up to 2.0 in localized areas off East Australia.

The ship's set data were analysed for a mean barotropic component, estimated as 5 ± 5 cm sec^{-1}, $045^{o} \pm 45^{o}$. The drift of the dynamic relief contours appeared to be 1 ± 1 cm sec^{-1} S, 5 ± 5 cm sec^{-1} E with some indication that the eastern front was expanding.

This type of analysis holds considerable promise for the future. If the ship were fitted with dual-axis electromagnetic log or a doppler sonar in addition to a satellite navigation system, reliable current averages over 1 to 5 hr periods could be obtained. Navigation systems in the future will be able to fix the ship's geographic position more accurately and more often. Thus more frequent current measurements could be made. If the ship's position were known continuously, a near-continuous readout of measured current would

be available. Such data, unlike those from a towed GEK, would include the barotropic component and would greatly enhance our knowledge of oceanography.

Acknowledgments

The author acknowledges the support of the officers and men of HMAS KIMBLA. The University of New South Wales Geophysics Department kindly loaned their satellite navigation system and the help of Mr B. Plummer during Trial 19/74 is gratefully acknowledged. Mr. V. Hardy of the Weapons Research Establishment assisted in the trial and Mr. J. Andrews of the same establishment assisted in the data reduction, calculated the values of dynamic height anomaly and has given much help to the author through many discussions. The author also acknowledges many helpful discussions with Dr. S. Godfrey of the CSIRO Division of Fisheries and Oceanography. Mr. A. R. Latham provided technical support for the project. This work was carried out under RANRL Project ANZUS Eddy and DST Task SASI 76/059.

References

1. Andrews, J.C. (1976). The Bathythermograph as a tool in gathering synoptic thermohaline data. *Aust. J. Mar. Freshwater Res.*, 27, 405-415.

2. Andrews, J.C. and P. Scully-Power (1976). The structure of an East Australian Current anticyclonic eddy. *J. Phys. Oceanogr.*, 6, 756-765.

3. Boland, F.M. and B.V. Hamon (1970). The East Australian Current, 1965-1968. *Deep-Sea Res.*, 17, 777-794.

4. Godfrey, J.S. (1973). Comparison of the East Australian Current with the western boundary flow in Bryan and Cox's (1968) numerical model ocean. *Deep-Sea Res.*, 20, 1059-1076.

5. Hamon, B.V. (1965). The East Australian Current, 1960-1964. *Deep-Sea Res.*, 12, 899-921.

6. Nilsson, C.S. (1977). Aust. RAN Research Laboratory. *The effect of weather on ship's speed.* (U). Tech. Note 4/77.

7. Nilsson, C.S., J.C. Andrews and P. Scully-Power (1977). Observations of eddy formation off East Australia. *J. Phys. Oceanogr.*, 7, 659-669.

8. Von Arx, W.S. (1962). *Introduction to Physical Oceanography*, Addison-Wesley, Reading.

APPENDIX

THE OBSERVED WEATHER DURING TRIAL 19/74

Time	Wind		Waves	Swell	
hr	°true	kn	ft	°true	ft
15	150	8	2	170	5
19	200	8	1	180	4
23	180	14	1	180	6
27	-	0	1	180	6
31	040	5	2	180	8
35	000	19	2	020	5
39	040	19	3	020	5
43	000	30	4	030	7
47	010	30	6	010	12
51	010	19	3	010	8
55	180	14	4	020	6
59	150	14	3	180	4
63	130	8	2	150	4
65	150	14	4	330	4
67	110	25	4	150	6
71	110	14	3	160	5
75	180	5	2	180	3
79	000	5	2	210	4
83	090	2	1	090	2
87	060	5	2	080	4
91	050	5	2	050	4
95	020	5	0	040	3
99	010	2	1	020	2
103	240	8	3	-	0
107	230	14	2	250	4
111	190	19	2	190	4
115	170	25	5	180	4
119	180	14	2	180	5
123	135	2	1	170	3

Original units are given (1 m = 3.28 ft)

TABLE 1

OBSERVED AND EXPECTED DRIFT DATA FOR TRIAL 19/74

Leg	Class	Δt hr	Observed Drift				Expected Drift		
			Dist. n.mi.	Dirn. °True	Speed kn	v_{dr} m.sec^{-1}	C_{δ} m.sec^{-1}	Dirn. °True	Dist. n.mi.
A-B	S	1.77	2.9	091	1.6	0.83	0.83	095	2.9
G-H$_{\perp}$	B	2.43	3.0	(116)	1.2	0.63	0.79	110	3.8
J-K	S	6.10	9.5	249	1.6	0.80	0.94	245	11.2
K-L	B	2.33	3.2	211	1.4	0.71	0.83	205	3.8
L-M	B	2.77	2.8	213	1.0	0.51	0.83	180	4.5
M-N	B	4.93	8.9	150	1.8	0.93	0.75	135	7.2
N-P	S	3.57	9.1	100	2.6	1.31	0.94	090	6.5
P-Q	B	1.97	4.7	083	2.4	1.22	0.75	080	2.9
Q-R	S	5.53	4.2	016	0.8	0.39	0.43	010	4.6
R-S	S	5.30	7.5	290	1.4	0.73	0.87	285	9.0
S-T	S	5.50	7.9	288	1.4	0.74	0.85	285	9.1
T-U	B	1.70	2.6	317	1.5	0.78	0.63	320	2.1
U-V	B	2.80	4.5	323	1.6	0.83	0.63	000	3.4
V-W$_{\perp}$	B	2.13	2.8	(006)	1.3	0.67	0.32	005	1.3
X-Y$_{\perp}$	B	1.77	2.8	(172)	1.6	0.80	0.50	175	1.7
Y-Z	B	1.77	4.0	191	2.3	1.17	0.68	170	2.4

$_{\perp}$ indicates normal component only.

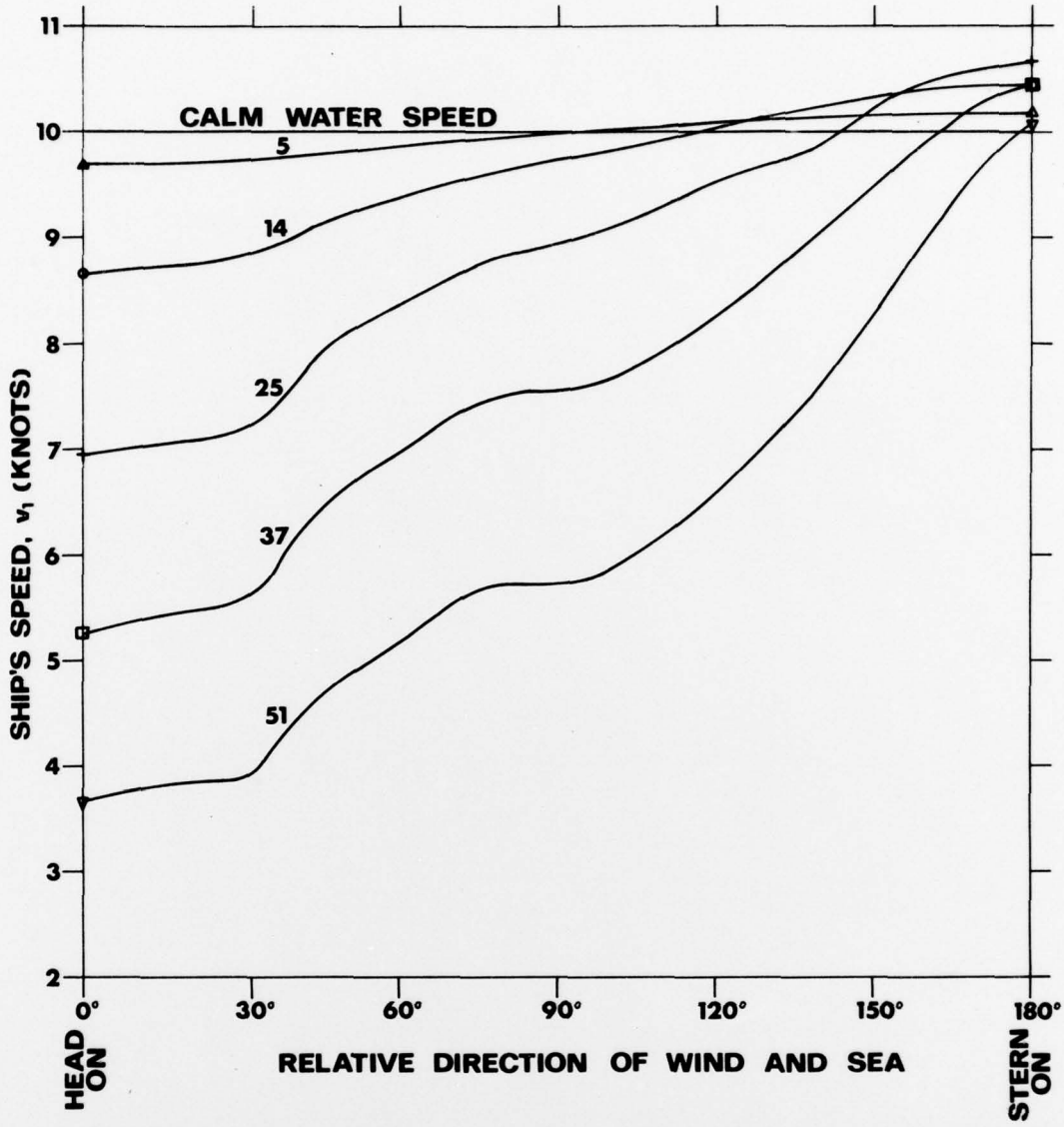

Fig.1. MODEL OF HMAS KIMBLA'S SPEED (AT 150 RPM) AS A FUNCTION OF WIND VELOCITY (KNOTS).

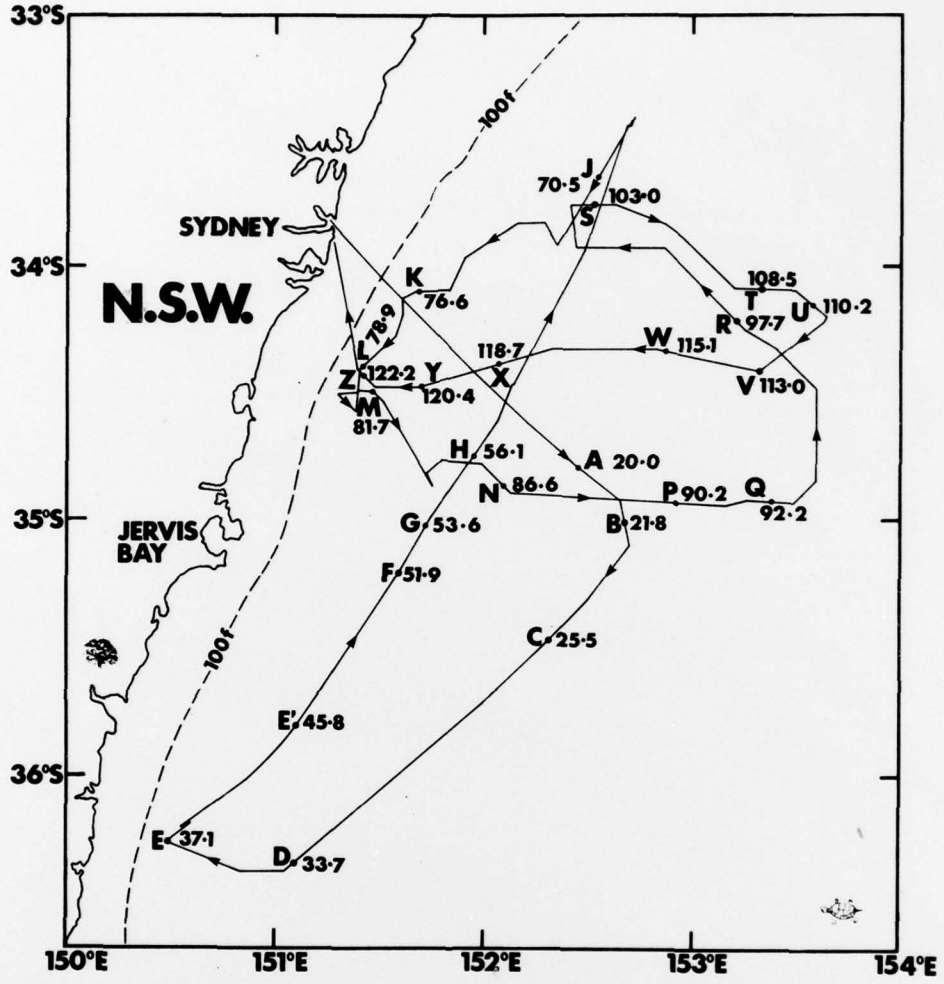

FIG. 2. SHIP'S TRACK, HMAS KIMBLA TRIAL 19/74, 8-13 DEC. 1974 (time in hr).

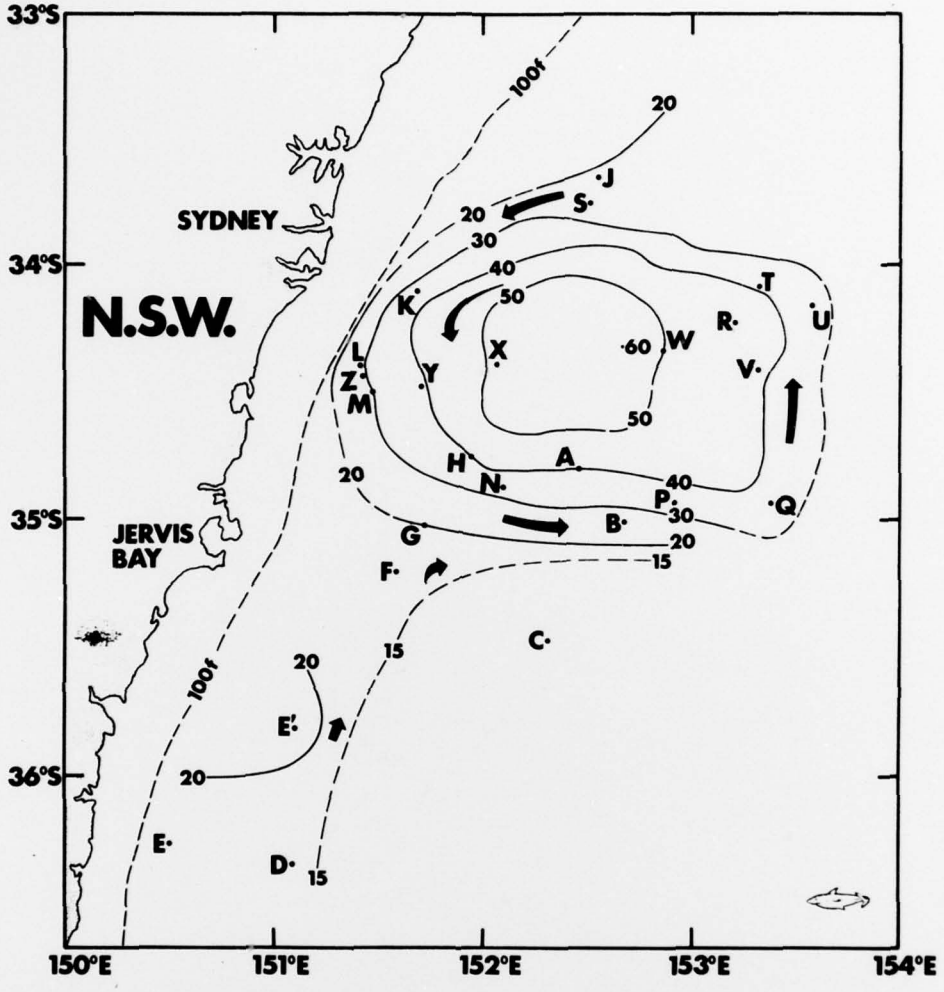

FIG. 3. DYNAMIC TOPOGRAPHY, D 0-900m (dyn. cm.)

HMAS KIMBLA TRIAL 19/74.

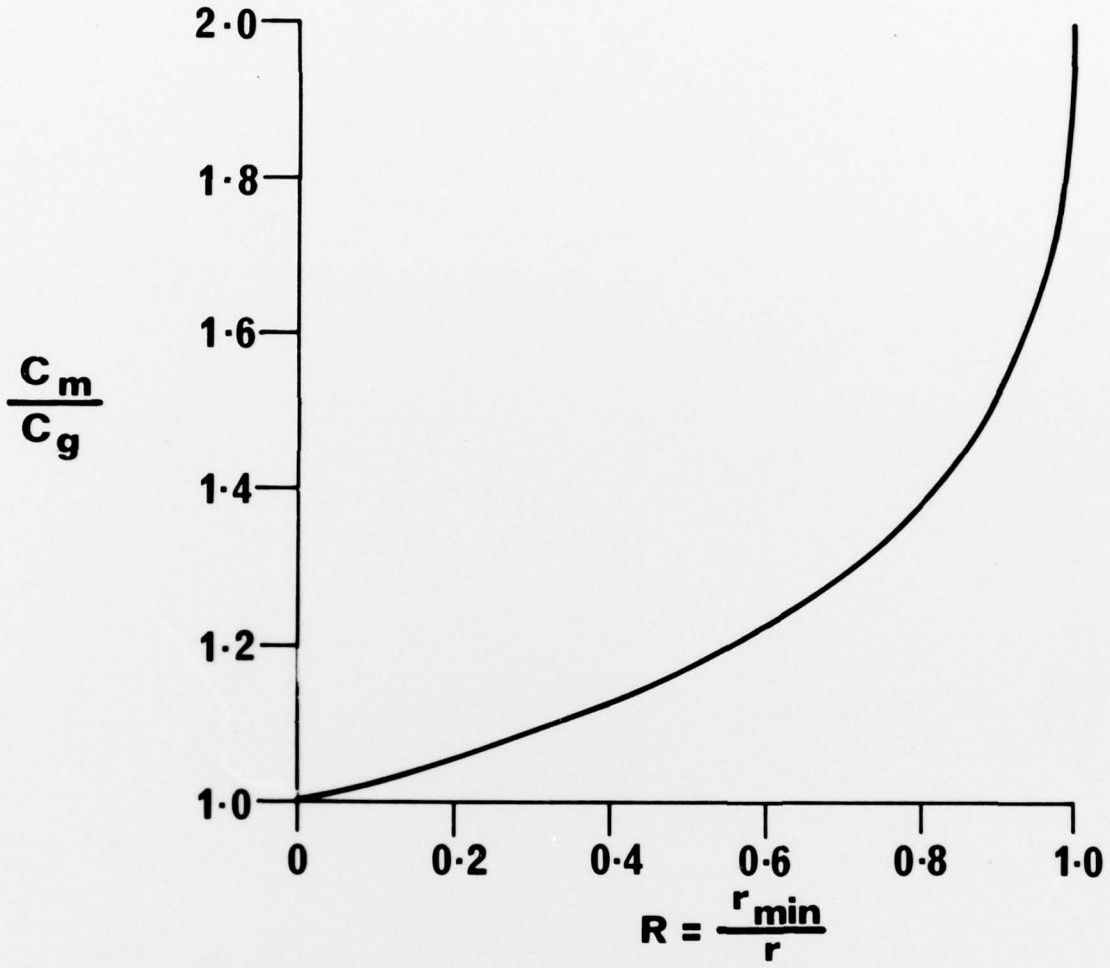

FIG.4. THE RATIO OF MEANDER TO GEOSTROPHIC SPEED AS A FUNCTION OF CURVATURE.